

## Article

# Effects of the Operational Parameters in a Coupled Process of Electrocoagulation and Advanced Oxidation in the Removal of Turbidity in Wastewater from a Curtember

Paul Alcocer-Meneses <sup>1</sup>, Angel Britaldo Cabrera-Salazar <sup>1</sup>, Juan Taumaturgo Medina-Collana <sup>1</sup>, Jimmy Aurelio Rosales-Huamani <sup>2,\*</sup>, Elmar Javier Franco-Gonzales <sup>2</sup> and Gladis Enith Reyna-Mendoza <sup>1</sup>

<sup>1</sup> Water Treatment Process Engineering Research Center, Faculty of Chemical Engineering, National University of Callao, Juan Pablo II 306 Avenue, Bellavista, Callao 07011, Peru

<sup>2</sup> Multidisciplinary Sensing, Universal Accessibility and Machine Learning Group, Faculty of Geological, Mining and Metallurgical Engineering, National University of Engineering, Lima 15333, Peru

\* Correspondence: jrosales@uni.edu.pe; Tel.: +51-1-381-5639

**Abstract:** The tannery industry during its process generates various polluting substances such as organic matter from the skin and chemical inputs, producing wastewater with a high concentration of turbidity. The objective of this research is to evaluate the most appropriate operational parameters of the coupled process of electrocoagulation and advanced oxidation to achieve the removal of turbidity in wastewater from a tannery in the riparian zone (tannery). This process uses a direct current source between perforated aluminum electrodes of circular geometry submerged in the effluent, which causes the dissolution of the aluminum plates. For our study, an electrocoagulation unit coupled to an ozone generator has been built at the laboratory level, where the influence of five factors (voltage, inlet flow to the reactor, initial turbidity, pH, and ozone flow) has been studied with three levels with regarding turbidity, using the Taguchi experimental methodology. The optimal conditions for the removal of turbidity were obtained at 10 volts, 7.5 pH, 360 L/h of wastewater recirculation flow rate; 2400 mg/h of ozone flow rate; and 1130 NTU of initial turbidity of the sample in 60 min of treatment reaching a removal of 99.75% of the turbidity. Under optimal conditions, the removal of chemical oxygen demand (COD) and biochemical oxygen demand (BOD) was determined, reaching a removal percentage of 33.2% of COD and 39.36% of BOD was achieved. Likewise, the degree of biodegradability of the organic load obtained increased from 0.467 to 0.553.

**Keywords:** electrocoagulation; tannery effluent; ozonation; optimization; turbidity removal; Taguchi



**Citation:** Alcocer-Meneses, P.; Cabrera-Salazar, A.B.; Medina-Collana, J.T.; Rosales-Huamani, J.A.; Franco-Gonzales, E.J.; Reyna-Mendoza, G.E. Effects of the Operational Parameters in a Coupled Process of Electrocoagulation and Advanced Oxidation in the Removal of Turbidity in Wastewater from a Curtember. *Appl. Sci.* **2022**, *12*, 8158. <https://doi.org/10.3390/app12168158>

Academic Editors: Amit Kumar, Santosh Subhash Palmate and Rituraj Shukla

Received: 28 May 2022

Accepted: 14 July 2022

Published: 15 August 2022

**Publisher's Note:** MDPI stays neutral with regard to jurisdictional claims in published maps and institutional affiliations.



**Copyright:** © 2022 by the authors. Licensee MDPI, Basel, Switzerland. This article is an open access article distributed under the terms and conditions of the Creative Commons Attribution (CC BY) license (<https://creativecommons.org/licenses/by/4.0/>).

## 1. Introduction

The leather trade can be an economic problem for developing countries that produce a good type of product from animal leather, such as footwear, luggage, and clothing. However, its production has a terribly high environmental footprint [1]. In addition, considering the enormous quantity and low biodegradability of the chemical products present in the productive cycle of tannery work, the wastewater from said process represents a great environmental and technological inconvenience [2]. In [3], the authors mentioned that the Electrocoagulation (EC) is often considered as an alternate treatment methodology with several advantages such as easy instrumentality, simple operation and automation, a brief retention time, low sludge production, and no chemical necessities.

Other studies have stated that Electrocoagulation mixtures and alternative technologies have been designed to treat high concentration organic waste material such as the textile trade and mixed industries [4,5]. In [6], mentioned that the use of EC as the only treatment process could face serious practical limitations, especially if the wastewater is highly contaminated. Therefore, there is a need for an efficient and relatively inexpensive treatment process. Due to this, the use of a post- or pre-treatment process with the EC

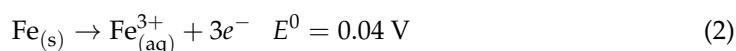
will improve its performance, as mentioned by several studies that have described more profitable combined treatment systems [6,7].

The authors of [8] published a review that includes EC combined with other treatment processes such as: electrocoagulation–ozone, electrocoagulation–adsorption, electrocoagulation–ultrasound, and electrocoagulation–pulses. In his work, the authors also mention about the performance of these combined systems.

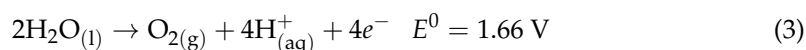
According to [9] Electrocoagulation (EC) is used in chemical science water treatment techniques where anode electrodes (aluminum, Al, or iron, Fe) area unit are dissolved in place, which promote coagulation and succeeding removals of pollutants and also the concurrent reduction of turbidity from water and wastewater. EC relies on the physical–chemical method of destabilization of mixture systems below the action of a right away current [10].

The electrodes dissolve according to Equations (1) and (2) to provide coagulant metal ions ( $\text{Al}^{3+}$  or  $\text{Fe}^{2+}/\text{Fe}^{3+}$ ) into the water, and these instantaneously carries rapid hydrolysis.

Anode reactions:

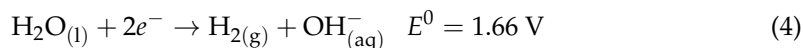


When the anode potential is sufficiently high, secondary reactions may occur, especially oxygen evolution, according to Equation (3)



Simultaneously with the anode reaction, water molecules  $\text{H}_2\text{O}$  break down at the cathode, producing hydrogen gas  $\text{H}_2$  and  $\text{OH}^{-}$  ions, according to Equation (4).

Cathode reaction:



The electrical energy applied to the anode dissolves the aluminum into the solution which then reacts with the hydroxyl ion from the cathode to form aluminum hydroxy. The most significant advantage of electrocoagulation is avoiding any addition of chemical substances thus reducing the likelihood of secondary pollution; the dosing of coagulator depends on the cell potential (or current density) applied [11]. Other advantages are the simple equipment, so requiring less maintenance and straightforward automation of the method [12].

Standard treatments for cloudiness removal have many disadvantages, such as the use of enormous amounts of chemicals and generating large amounts of sludge that causes disposal issues and therefore the loss of water. Then in [13] mentioned that the combination of ultrasound technique with different processes such as electrocoagulation, electro-Fenton, and electrooxidation could be important to achieve effective decomposition of organic contaminants in wastewater. Independently in [14] mentioned the integrated sonoelectro-Fenton (SEF) method could be a novel methodology for the removal of paracetamol (PCT) waste material from liquid solutions through synthesized iron ore ( $\text{Fe}_2\text{O}_3$ ) nanoparticles.

The novelty of our study was the design of the electrocoagulation cell with perforated plates installed vertically, improving the mixture of ozone with the residual water and the ions generated by the electrodes. In this way, reducing areas of stagnation in the electrocoagulation cell that produce passivation of the electrodes, causing a decrease in the efficiency of the process.

The objective of this study was to examine the treatment of wastewater from the tanning industry, through the electrocoagulation process, the impact of the factors electrical potential, feed flow, initial concentration of turbidity, pH, and ozone flow on the percentage reduction of turbidity and energy consumption, based on the Taguchi methodology.

## 2. Materials and Methods

### 2.1. Effluent Sample Collection

The samples were collected from the operations corresponding to the riparian zone (pre-soaking, main soaking, peeling, descaling, and purging or delivery), from the tannery located in the district of Ate Vitarte, Lima (Peru). Each sample was collected and then homogenized and allowed to stand for 3 h. These samples came from a process of transformation of sheep skins preserved with salt, with hair destruction technology.

A part of the sample was sent to a specialized laboratory, applying the corresponding monitoring protocols to know the physicochemical characteristics, as illustrated in Table 1.

**Table 1.** Some of the physicochemical characteristics of the wastewater of the riparian zone.

Parameters	Unit	Value
pH		9.43
Turbidity	NTU	1130
Chemical oxygen demand	mg/L	2638
Biological oxygen demand	mg/L	1232
Oils and fats	mg/L	15.1
Ammonia nitrogen	NH <sup>3+</sup> -N mg/L	88.85
Sulfides	S = mg/L	21.4
Fecal coliforms	NMP/100 mL	<1.8
Aluminum	mg/L	0.29

### 2.2. Analytical Methods

The turbidity was measured by Ezodo model TUB-430, turbidimeter, to determine the pH, conductivity and total dissolved solids, the Multiparameter equipment (pH, EC, TDS, T °C), HANNA brand was used. To determine the voltage and current intensity, the Digital Hook Multimeter (amps, voltage, temperature, etc.) was used.

### 2.3. Design of Experiment

The optimization of wastewater turbidity removal using Aluminum electrodes was performed using the Taguchi Design. Five important factors such as voltage, feed flow, effluent concentration, pH, and ozone flow were used as independent variables where their combined effects were examined, while the percentage of turbidity removal was the dependent variable.

This was performed to determine the best conditions for the optimum removal of turbidity from the wastewater. The experimental design involves varying the independent variable at three different levels (−1, 0, +1). The experimental range and levels of the independent variables are presented in Table 2. In this work, a set of 27 experiments with two replicates, the mean shown in Table 3. Where the levels of the applied electrical potential were acquired from the work developed by [15] and to select the pH range the research work provided by [16] was taken.

The interactive effects of the independent (process) variables on the dependent variable (response) were examined using the analysis of variance (ANOVA) as shown in Table 4.

**Table 2.** Experimental range and levels of independent variables used in this study.

Factors	Unit	Notation	Levels		
			Low	Medium	High
Voltage	V	X1	4	7	10
Feed flow	L/h	X2	240	300	360
Turbidity	NTU	X3	375	580	1130
pH		X4	4.0	7.5	10.8
Ozone flow	mg/h	X5	900	1500	2400

**Table 3.** Presents the results of the 27 experiments carried out using the Taguchi methodology of five factors at three levels under study.

N° Tests	Factors						Response							
	X1 (V) Voltage	X2 (L/h) Feed Flow	X3 (NTU) Turbidity	X4 (pH)	X5 (mg/h) Ozone	Flow	Turbidity (NTU)	% Turbidity	Reduction	Faraday Aluminum	Dough (g)	Energy Consumed	in the Cell	(KWh/m <sup>3</sup> )
1	4	240	375	4	900		471.4	58.28		0.1176			175.17823	
2	4	240	375	4	1500		487.8	56.83		0.0535			85.34855	
3	4	240	375	4	2400		483.6	57.2		0.0471			76.356466	
4	4	300	580	7.5	900		48.7	91.65		0.0279			45.541531	
5	4	300	580	7.5	1500		55.5	90.48		0.0314			50.222793	
6	4	300	580	7.5	2400		52.3	91.03		0.0397			63.811338	
7	4	360	1130	10.8	900		88.3	76.45		0.0246			37.127518	
8	4	360	1130	10.8	1500		91.2	75.68		0.0275			43.868429	
9	4	360	1130	10.8	2400		87.1	76.77		0.0294			46.751746	
10	7	240	580	10.8	900		135.2	76.49		0.2093			657.31997	
11	7	240	580	10.8	1500		145.1	74.77		0.1539			499.21802	
12	7	240	580	10.8	2400		139.7	75.7		0.1726			551.08302	
13	7	300	1130	4	900		3.2	99.14		0.1111			365.33785	
14	7	300	1130	4	1500		1.3	99.65		0.1135			362.05164	
15	7	300	1130	4	2400		0	100		0.136			421.1065	
16	7	360	375	7.5	900		17.5	98.45		0.1822			570.44258	
17	7	360	375	7.5	1500		13.8	98.78		0.1936			604.95181	
18	7	360	375	7.5	2400		15.2	98.66		0.1485			479.17558	
19	10	240	1130	7.5	900		7.2	98.11		0.1402			652.35772	
20	10	240	1130	7.5	1500		5.2	98.64		0.1546			748.96169	
21	10	240	1130	7.5	2400		2.8	99.27		0.1492			712.034	
22	10	300	375	10.8	900		207	81.63		0.2704			1178.6499	
23	10	300	375	10.8	1500		195.2	82.68		0.2993			1310.3554	
24	10	300	375	10.8	2400		198	82.43		0.153			726.03864	
25	10	360	580	4	900		0	100		0.238			1060.6992	
26	10	360	580	4	1500		1.2	99.79		0.2312			1029.1543	
27	10	360	580	4	2400		1.57	99.73		0.2371			1042.1303	

**Table 4.** Analysis of variance (ANOVA).

Source	GL	SC Sec.	Contribution	SC Ajust.	MC Ajust.	Value F	Value p
Model	14	5252.01	99.94%	5252.01	375.14	1337.59	0.000
Linear	5	3347.2	63.69%	3392.4	678.48	2419.14	0.000
X1	1	1669.48	31.77%	1560.97	1560.97	5565.7	0.000
X2	1	924.79	17.60%	919.82	919.82	3279.66	0.000
X3	1	514.58	9.79%	656.93	656.93	2342.3	0.000
X4	1	238.29	4.53%	254.67	254.67	908.05	0.000
X5	1	0.06	0.00%	0.06	0.06	0.23	0.643
Square	5	1903.28	36.22%	1903.28	380.66	1357.24	0.000
(X1) <sup>2</sup>	1	193.78	3.69%	193.78	193.78	690.95	0.000
(X2) <sup>2</sup>	1	256.89	4.89%	256.89	256.89	915.95	0.000
(X3) <sup>2</sup>	1	210.76	4.01%	210.76	210.76	751.48	0.000
(X4) <sup>2</sup>	1	1241.12	23.62%	1241.12	1241.12	4425.26	0.000
(X5) <sup>2</sup>	1	0.72	0.01%	0.72	0.72	2.56	0.135
Error	12	3.37	0.06%	3.37	0.28		
Total	26	5255.38	100.00%				

#### 2.4. Electrocoagulation Reactor

The EC experiments were performed by a batch process using a 7 L capacity of a cylindrical reactor, the configuration (Figure 1) of the electrochemical reactor has a cylindrical shape, aluminum electrodes were used both for the anode and for the circular cathode (Perforated plates), we work with a configuration of parallel monopolar electrodes, with a separation of 1 cm as mentioned in [17–19], and the specific area of each electrode was 0.014 cm<sup>2</sup>. Each electrode was 10 cm (diameter) with 10 holes of 10 mm diameter each, by 0.3 cm (thickness), the number of electrodes used were four. The EC cell was configured for the vertical water flow of the feed water that was delivered by a peristaltic pump. Accessory (ACC) power supply was connected (0–15 volts). Before installation in the EC unit, each plate was weighed to allow the calculation of the mass consumed after the tests. Each experiment was continued for 60 min, which was considered enough to achieve a stable operation. Ozone was coupled to the system by means of venturi, the ozone generating equipment has a capacity of (0 to 3 g O<sub>3</sub>/h).

All experiments were performed at room temperature (nominally 20 °C). After the seating time elapsed, the samples were removed from a depth of 2 cm using a syringe and measured using the turbidity meter. The electrodes were cleaned in a solution of low concentration hydrochloric acid (0.04 M) and another caustic soda solution (0.08 M) to remove the remains stuck on the surface of the electrodes; they were finally washed with distilled water for reuse. The arrangement of the electrodes consisted of two cathodes that were interspersed with two anodes connected by stainless steel rods to other arranged and then the samples were periodically taken every 10 min for the measurement of turbidity. The power was supplied to the electrodes with a Direct Current (DC) power supply.

An improvement over other reported works [15,20,21] is the configuration of the experimental equipment used. In this investigation, an electrocoagulation cell with perforated circular electrodes has been built. This design allows for improved mixing, longer residence time for the effluent and ozone. therefore the mechanisms used in this hybrid process are improved such as sedimentation [15,22]. A disadvantage compared to other configurations of electrocoagulation cells is the maintenance of the electrodes, which is relatively easy.

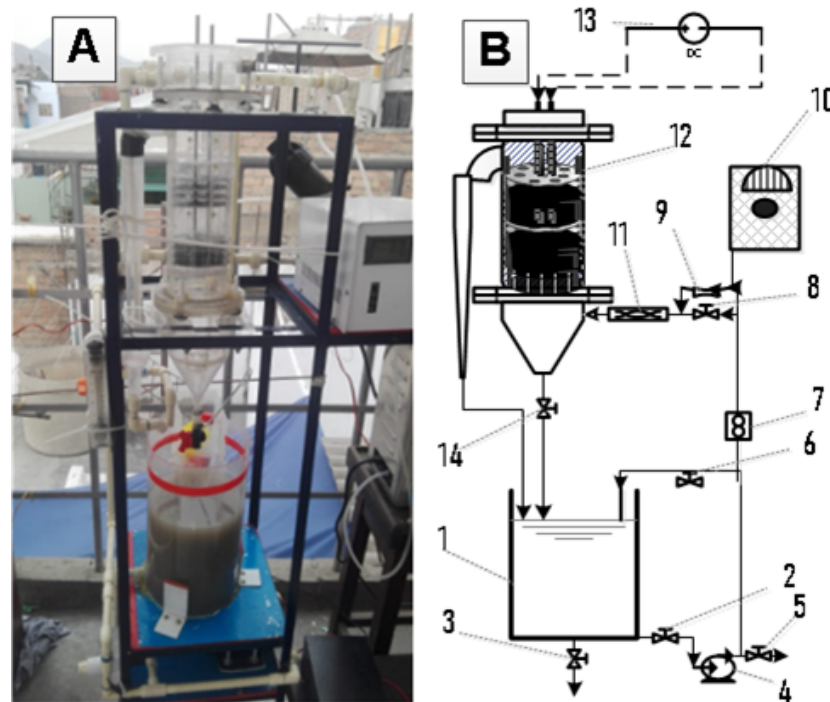


**Figure 1.** Electrocoagulation and ozone experimental module. (A) Photograph of the experimental module doing preliminary tests. The sample is fed to tank 1, followed by the sample being pumped through the flow meter, followed by the Venturi system, dynamic mixer until reaching the electrolytic reactor, once the system is filled again the sample returns to the tank. (B) Module diagram, where 1 is the deposit; 2, 3, 5, 6, 8, and 14 stopcocks; 4 recirculation pump; 7 flow meter; 9 Venturi; 10 ozone generator; 11 dynamic mixer; 12 electrocoagulation reactor and 13 current rectifier.

### 2.5. The Main Calculations of Electrocoagulation Process

The reduction rate of turbidity, expressed in percentage “ $T$ ” (%), was calculated using Equation (5).

$$T(\%) = \left( \frac{T_i - T_f}{T_i} \right) \times 100\% \quad (5)$$

where  $T_i$  and  $T_f$  represent initial and final turbidity, respectively. Electrical energy consumption is a very important economical parameter in the electrocoagulation process. The electrical energy consumption was calculated using the following Equation (6) [23].

$$C.E. = \frac{U}{Vm} \int_0^{3600} I(t) dt \quad (6)$$

$C.E.$  is the energy consumption ( $\text{kWh}/\text{m}^3$ )

$U$  is the applied voltage (V)

$Vm$  is the treated volume of the sample (L).

The integral represents the intensity value multiplied with time in seconds.

The amount of dissolved electrode was calculated theoretically using Faraday’s law [24], through the following Equation (7).

$$m = \frac{M}{nF} \int_{t. \text{ inicial}}^{t. \text{ final}} I(t) dt \quad (7)$$

$m$  is the aluminum mass (g) in the electrolytic cell

$I$  is the intensity of the current (A)

$t$  is the electrocoagulation time (s),  $M$  is the molecular weight of the anode (g/mol)

$z$  is The chemical equivalence,  $F$  is the faraday constant (96,500 c/mol)

( $M_{Al} = 26,982 \text{ g/mol}$ )

$n$  is the valence of the ions of the electrode material ( $n_{Al} = 3.0$ ).

### 3. Results

The results of our experiment are shown below. Complementing the results of Table 3, the standard deviation has been evaluated with respect to the mean of the percentage of turbidity removal and Energy consumption whose results are shown in Table 5. Then we show the physicochemical parameters obtained in Table 6.

**Table 5.** Standard deviation of percent turbidity removal and energy consumption and Energy consumption.

Response	N	Statistical Minimum	Statistical Maximum	Mean	Standard Error	Standard Deviation
Turbidity removal percentage	27	56.83	100	86.6033	2.736	14.217
Energy consumption (KW/m <sup>3</sup> )	27	0.037	1.310	0.503	0.075	0.390

**Table 6.** Results of the physicochemical characterization of the treated sample.

Parameters	Unit	Value
pH		8.6
Turbidity	NTU	2.8
Chemical oxygen demand	mg/L	876
Biological oxygen demand	mg/L	485
Oils and fats	mg/L	<1.2
Ammonia nitrogen	NH <sup>3+</sup> -N mg/L	32.75
Sulfides	S = mg/L	<0.002
Fecal coliforms	NMP/100 mL	<1.8
Aluminum	mg/L	44.06

#### 3.1. Main Effect of Variables

The main effect plots for the six operating variables are given in Figure 2. The main effects of the tested variables were calculated by averaging the experiment results achieved at each level for each variable. This plot was obtained from Table 3 and is used to visualize the relation between variables and the output response.

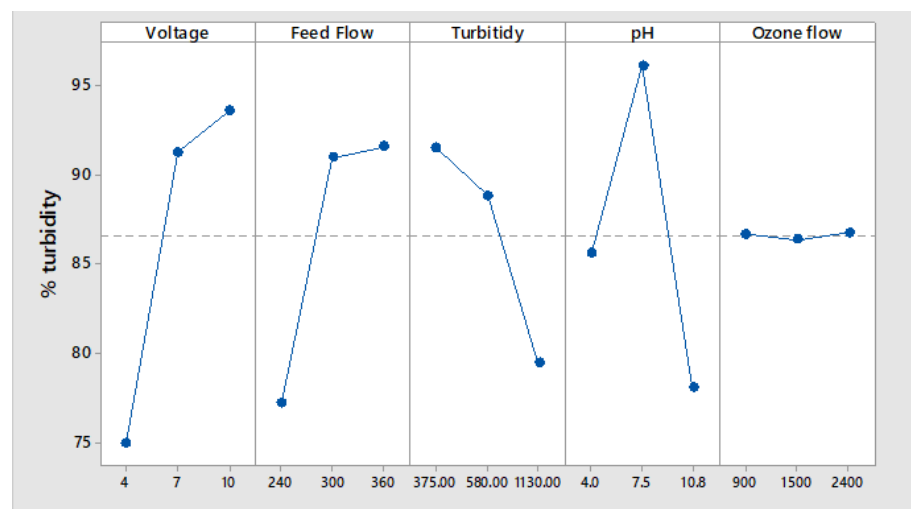


**Figure 2.** The effects of the operating variables on the mean turbidity removal percentage.

### 3.1.1. Comparison of Ozonation, Electrocoagulation, and Ozone-Assisted Electrocoagulation

From Figure 3 we observe that for the initial turbidity of 655 NTU of the sample, when the process is hybrid (electrocoagulation and ozone), a turbidity of 4.19 NTU is reached (99.36% turbidity removal). In the electrocoagulation process, a turbidity of 18.34 NTU (97.2%) is obtained and through ozone up to 196.6 NTU (69.98%) is reached, therefore it is concluded that the hybrid and electrocoagulation process reach yields above 97% for removal of turbidity. We also observed that the removal of turbidity in the three processes is achieved in the first 20 initial minutes of treatment. In the work of [25] indicated that the combined electrocoagulation/ozonation process improved both the degradation rate and the maximum removal of COD compared to the electrocoagulation and ozonation processes alone.

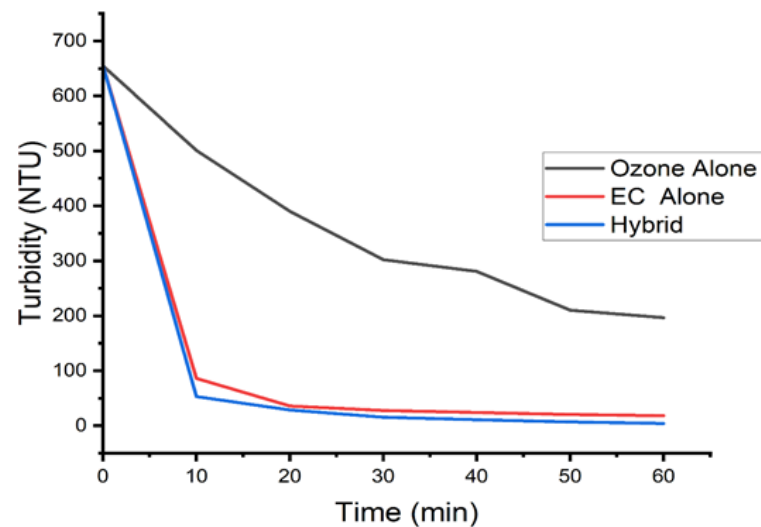


**Figure 3.** Turbidity reduction for separate processes such as pure ozone, electrocoagulation and coupled process of EC/O<sub>3</sub>, operated at conditions of 10.0 volts, feed flow 360 L/h, O<sub>3</sub> flow 2400 mg/h, pH 6.89, and initial turbidity of 655 NTU.

### 3.1.2. Initial pH Effect

From Table 3, trials 1, 4, 10, 20, 24, and 27 have been plotted as they are the most representative. Then it is observed from Figure 4 that for experiments 1 and 10 the pH of the sample increases with the treatment time. For experience 27, a pH of 8.21 is reached and is attributed mainly to the increase in electrical potential (10 volts). When the initial pH is 7.5 for experiences 4 and 20, the increase is not very significant, reaching a final value of 8.54. Finally, when the sample has an initial pH of 10.8 in tests 10 and 24, a decrease is observed, reaching a value of 9.21.

The tannery industry generates effluents with a wide pH range, from pH = 3.5 to pH = 11; on the other hand, studies show that pH has a significant impact on electrocoagulation performance. The increase in pH is a consequence of the formation of Al<sup>3+</sup> which precipitates due to the presence of other anions, as well as the precipitation of aluminum hydroxide; however when the pH starts at alkaline, the decrease in pH is the result of the formation of Al(OH)<sub>4</sub><sup>-1</sup> [26].

### 3.1.3. Effect of Initial Turbidity

According to Figure 5B, a greater reduction in turbidity is observed as the initial turbidity is less than 1130 NTU, this behavior could be explained because the amount of flocs formed is sufficient for their adsorption and thus quickly decrease turbidity. This trend is also deduced from Faraday's law, which states that Al<sup>3+</sup> released to the solution for the same applied solution is constant [27].

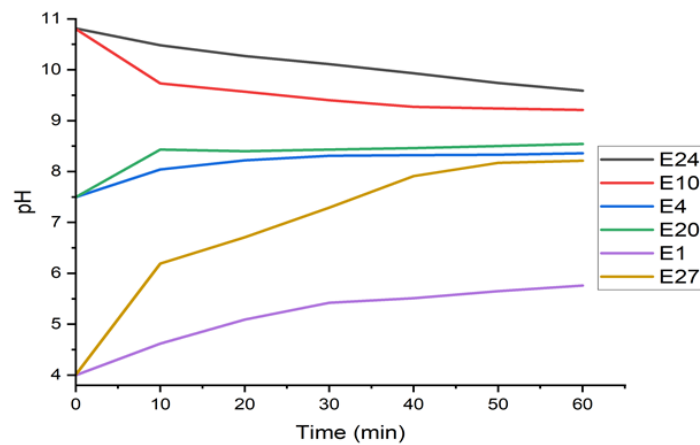


Figure 4. Variation of the pH in the time of treatment by electrocoagulation/O<sub>3</sub>.

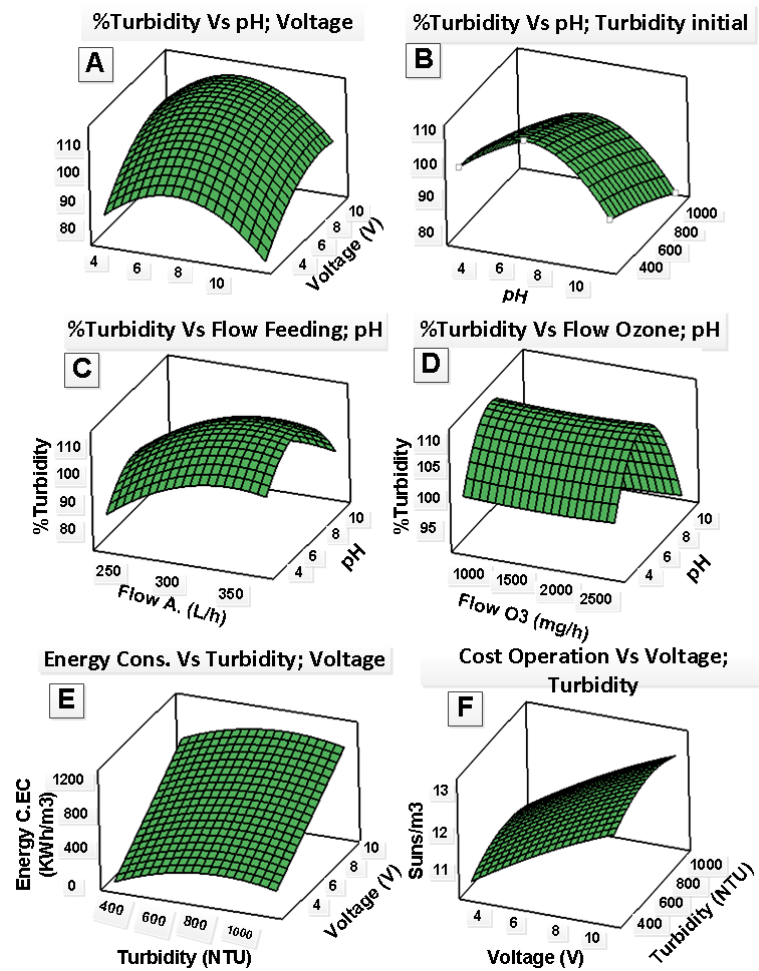
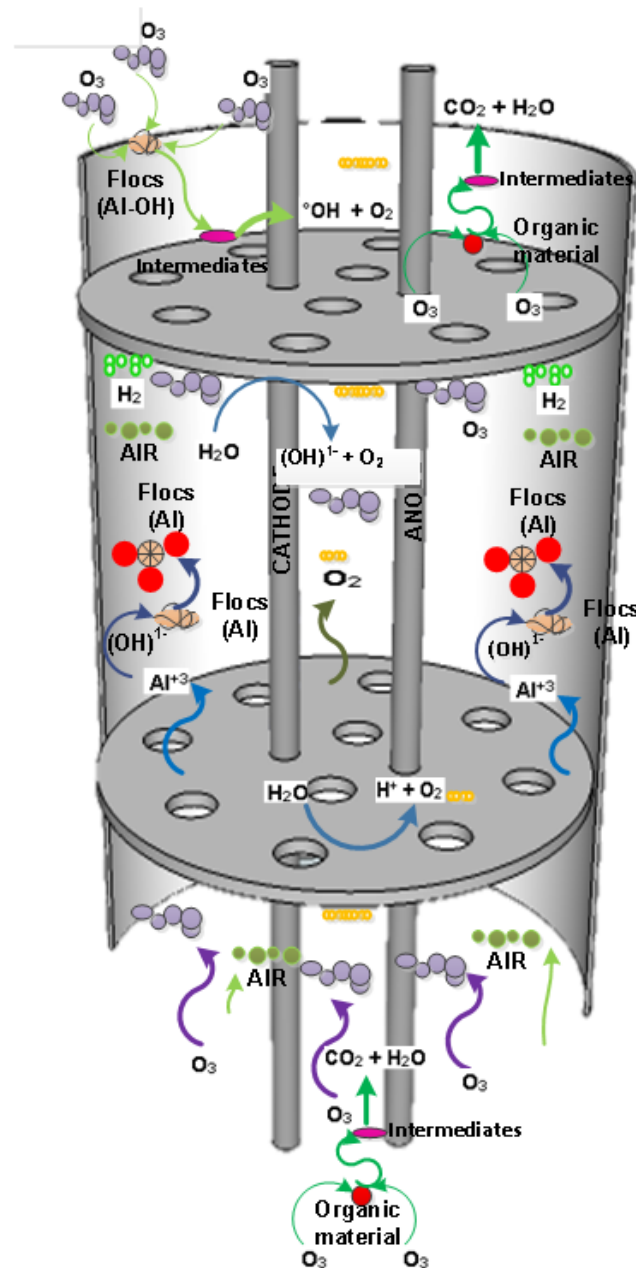


Figure 5. Representation of the effect of operational variables on % reduction in turbidity, energy consumed in the electrolytic cell, and operational cost of the module. (A) Variation of the pH and voltage variables against % turbidity for fixed values of 300 L/h, 752.5 NTU, and 1650 mg/h. (B) Variability of pH and initial turbidity versus % turbidity for fixed values of 6.5 volts, 300 L/h and 1650 mg/h of O<sub>3</sub> flow. (C) pH and feed flow variability versus % turbidity for fixed values of 6.5 volts, 752.5 NTU, and 1650 mg/h O<sub>3</sub> flow. (D) Ozone and pH flow variability versus % turbidity for fixed values of 6.5 volts, 300 L/h, and 752.5 NTU. (E) Variability of initial turbidity and voltage versus energy consumption in the electrocoagulation cell for fixed values of 300 L/h, 7.4 pH, and 1650 mg/h of O<sub>3</sub> flow. (F) Variability of voltage and initial turbidity against the cost of the built module for fixed values of 300 L/h, 7.4 pH, and 1650 mg/h of O<sub>3</sub> flow.

The proposed mechanism for the reduction of turbidity by means of the hybrid system of electrocoagulation and ozone is shown in Figure 6. This consists of destabilizing the colloidal particles and forming larger flocs, in which the contaminants are trapped and these flocs can be separated from the solution by flotation or sedimentation [28]. The dissolved air flotation mechanism is effective in reducing the organic load [29] and dissolved ozone flotation gives efficient results in the removal of suspended solids [30,31]. For soluble contaminants, aluminum-based coagulants can act as catalysts for ozone and generate hydroxyl formation [22] and also oxidize surface functional groups of colloidal contaminants that promote colloid aggregation.



**Figure 6.** Mechanism of hydroxyl formation.

#### 3.1.4. Feed Flow Effect

According to Figure 5C, as the feed flow increases (240 to 360 L/h) there is an increase in the reduction of turbidity, this could be attributed as the feed flow increases towards the reactor, there is a greater formation of bubbles, this is influenced by the principle of

hydrodynamic cavitation that forms in the Venturi tube [32]. As a consequence, the flotation mechanism predominates to reduce turbidity, this formation of bubbles increases when working under acidic conditions, forming two phases (80% foam and 20% liquid) [33]. However, this generation of bubbles generates a problem in the electrodes (activation polarization), generating an increase in voltage and a decrease in electrical current, thus an increase in energy consumption [34].

### 3.1.5. Ozone Flow Effect

Ozone flow is one of the factors that has the least influence on reducing turbidity, as can be seen in Figure 5D. Furthermore, in Figure 2, we observe that the mass flow of ozone does not have much influence on the removal of turbidity. In [35], mentioned that for the activation of ozone and its transformation into hydroxide ion ( $\text{OH}^-$ ), it is achieved through electroreduction, which in this case would help in the oxidation either directly or indirectly to the components present in the effluent (organic matter, nitrates, sulfides, etc.). To oxidize the sulfur, ozone is an alternative to the traditional ions ( $\text{Fe}^{2+}$ ,  $\text{O}_2$ , etc.), as verified in the research work [36].

## 4. Discussion

When evaluating the five operational parameters against the reduction of turbidity according to Figure 2, it is shown that the factor with the greatest influence is the voltage, corroborating it in Table 4 of ANOVA due to its greater contribution with respect to the other parameters. By increasing the potential values from 4 to 10 volts as seen in Figure 5A, it was possible to increase the percentage of turbidity reduction reaching 56.83% and 100%, a growing effect in the elimination of turbidity. This originated effect is analogous to those reported in [37], where they worked at 6, 8.5 and 10 volts, for one hour of treatment on grey water, reaching a reduction of 68%, 73%, and 86% respectively.

On the other hand, the effect on removal is due to the increase in particle size as a function of time, studied by [38], where he reported that in a synthetic sample of kaolinite, the size formed is affected as the voltage and time are increased, allowing the generation of a higher sedimentation rate of the particles.

This ascending effect of the voltage on the turbidity can also be seen in the report presented by [39], they worked in the range of 2.9 to 11.7  $\text{mA}/\text{cm}^2$ , for a time of 14 min on water. residues from car washes, achieving close to a 96% reduction in turbidity. On the other hand, the work presented by [15], also reported the influence of the applied potential on turbidity, where they evaluated 4 voltage levels for a period of 15 min such as: 2, 5, 10, and 15 V, achieving a reduction 83% for voltage 2 and 92% for 15 volts; therefore, as stated [40], the applied voltage is an influential and important parameter. As a main step, it ensures the production of  $\text{Al}^{3+}$  ion coagulants as a result of electrolytic oxidation of the electrode. Table 7 shows the results.

**Table 7.** Effect of the applied potential difference on the removal of the turbidity.

Electric Potential (V)	Turbidity (%)
2	83
5	90
10	91
15	92

From Table 3 we generate Figure 7 which shows the effect of the process parameters with respect to energy consumption in  $\text{kWh}/\text{m}^3$ . From said figure we observe that the average energy consumption in the 27 experiments was  $0.5 \text{ kWh}/\text{m}^3$ .

In addition, the factor with the greatest influence was the electrical potential applied to the electrocoagulation cell, as indicated by the diagram, the lowest energy consumption (0.069) was obtained with the electrical potential at 4 volts and the highest energy consump-

tion (0.94) was obtained at an electrical potential of 10 volts. Likewise, it is observed that turbidity has a significant influence on energy consumption at the high level, 0.376 kWh/m<sup>3</sup> is consumed, whose value is below the average.

In the study carried out by [15], about the reduction of turbidity and chromium content in tannery wastewater by electrocoagulation process using aluminum electrodes at an electrical potential of 10 volts, pH of 6.1, and a time of 90 min. The authors obtained an energy consumption of 1.5 kWh/m<sup>3</sup>, which is quite close to that obtained in our present study.

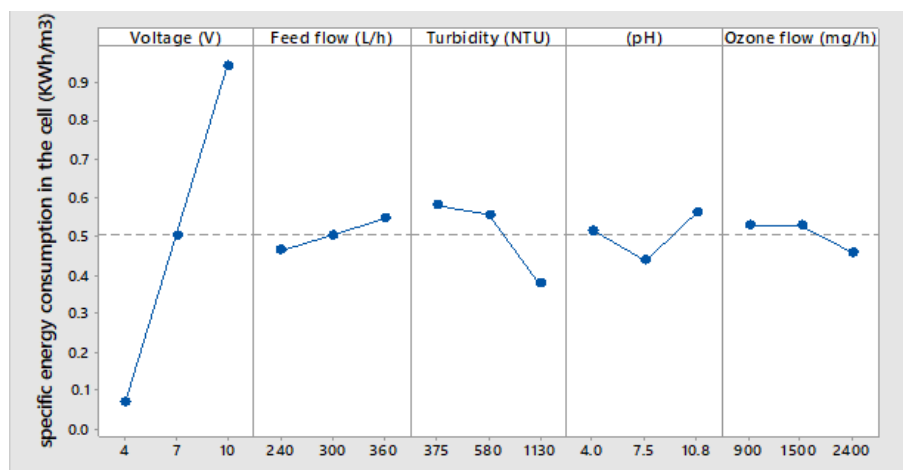


**Figure 7.** Effect of process parameters on specific energy consumption.

## 5. Conclusions

The coupled process of electrocoagulation with ozone was successfully tested in the treatment of wastewater from a tannery from the riparian zone. Parameters such as applied voltage potential, feed flow, initial turbidity concentration, pH, and ozone flux were studied on the percentage of turbidity reduction and energy consumption in the electrocoagulation cell. It was found that parameters have the greatest influence on turbidity reduction and the effects separately of each process such as ozone, electrocoagulation and ozone-assisted electrocoagulation on turbidity.

The result showed that the factor that has the greatest influence on reducing turbidity is voltage. The present study showed that the coupled electrocoagulation and ozone system reduced more turbidity than the processes alone. The optimal conditions for the removal of turbidity, Chemical Oxygen Demand (COD) and Biochemical Oxygen Demand (BOD) were obtained at 10 volts, 7.5 pH, 360 L/h of wastewater recirculation flow, 2400 mg/h of ozone flow, and 1130 NTU of initial turbidity of the sample in 60 min of treatment. Finally, under these conditions, a removal of 99.75% of turbidity, 33.2% of COD, and 39.36% of BOD was achieved. Likewise, the degree of biodegradability of the organic load obtained increased from 0.467 to 0.553.

**Author Contributions:** Conceptualization, P.A.-M.; Data curation, A.B.C.-S.; Investigation, J.A.R.-H.; Project administration, A.B.C.-S.; Software, J.T.M.-C.; Validation, P.A.-M.; Writing—original draft, E.J.F.-G.; Writing—review & editing, G.E.R.-M. All authors have read and agreed to the published version of the manuscript.

**Funding:** This research received no external funding.

**Conflicts of Interest:** The authors declare no conflicts of interest.

## References

1. Villaseñor-Basulto, D.L.; Picos-Benítez, A.; Pacheco-Alvarez, M.; Pérez, T.; Bandala, E.R.; Peralta-Hernández, J.M. Tannery wastewater treatment using combined electrocoagulation and electro-Fenton processes. *J. Environ. Chem. Eng.* **2022**, *10*, 107290. [[CrossRef](#)]
2. Di Iaconi, C.; Lopez, A.; Ramadori, R.; Di Pinto, A.; Passino, R. Combined chemical and biological degradation of tannery wastewater by a periodic submerged filter (SBBR). *Water Res.* **2002**, *36*, 2205–2214. [[CrossRef](#)]
3. Varank, G.; Erkan, H.; Yazycy, S.; Demir, A.; Engin, G. Electrocoagulation of tannery wastewater using monopolar electrodes: process optimization by response surface methodology. *Winter* **2014**, *8*, 165–1890.
4. Chanikya, P.; Nidheesh, P.; Babu, D.S.; Gopinath, A.; Kumar, M.S. Treatment of dyeing wastewater by combined sulfate radical based electrochemical advanced oxidation and electrocoagulation processes. *Sep. Purif. Technol.* **2021**, *254*, 117570. [[CrossRef](#)]
5. Nidheesh, P.; Kumar, A.; Babu, D.S.; Scaria, J.; Kumar, M.S. Treatment of mixed industrial wastewater by electrocoagulation and indirect electrochemical oxidation. *Chemosphere* **2020**, *251*, 126437. [[CrossRef](#)]
6. Al-Qodah, Z.; Tawalbeh, M.; Al-Shannag, M.; Al-Anber, Z.; Bani-Melhem, K. Combined electrocoagulation processes as a novel approach for enhanced pollutants removal: A state-of-the-art review. *Sci. Total. Environ.* **2020**, *744*, 140806. [[CrossRef](#)]
7. GilPavas, E.; Dobrosz-Gómez, I.; Gómez-García, M.Á. Optimization and toxicity assessment of a combined electrocoagulation,  $H_2O_2/Fe^{2+}/UV$  and activated carbon adsorption for textile wastewater treatment. *Sci. Total. Environ.* **2019**, *651*, 551–560. [[CrossRef](#)]
8. Barrera-Díaz, C.E.; Roa-Morales, G.; Hernández, P.B.; Fernandez-Marchante, C.M.; Rodrigo, M.A. Enhanced electrocoagulation: New approaches to improve the electrochemical process. *J. Electrochem. Sci. Eng.* **2014**, *4*, 285–296. [[CrossRef](#)]
9. Kuokkanen, V.; Kuokkanen, M.; Hynynen, I.; Kuokkanen, T. Electrocoagulation treatment of metallurgical industry wastewater—A laboratory scale batch and pilot scale continuous study. *Hydrometallurgy* **2021**, *202*, 105596. [[CrossRef](#)]
10. Sillanpää, M.; Shestakova, M. *Electrochemical Water Treatment Methods: Fundamentals, Methods and Full Scale Applications*; Butterworth-Heinemann: Oxford, UK, 2017.
11. Mollah, M.Y.; Morkovsky, P.; Gomes, J.A.; Kesmez, M.; Parga, J.; Cocke, D.L. Fundamentals, present and future perspectives of electrocoagulation. *J. Hazard. Mater.* **2004**, *114*, 199–210. [[CrossRef](#)]
12. Mollah, M.Y.A.; Schennach, R.; Parga, J.R.; Cocke, D.L. Electrocoagulation (EC)—Science and applications. *J. Hazard. Mater.* **2001**, *84*, 29–41. [[CrossRef](#)]
13. Hassani, A.; Malhotra, M.; Karim, A.V.; Krishnan, S.; Nidheesh, P. Recent progress on ultrasound-assisted electrochemical processes: A review on mechanism, reactor strategies, and applications for wastewater treatment. *Environ. Res.* **2022**, *205*, 112463. [[CrossRef](#)] [[PubMed](#)]
14. Ghanbari, F.; Hassani, A.; Waclawek, S.; Wang, Z.; Matyszczyk, G.; Lin, K.Y.A.; Dolatabadi, M. Insights into paracetamol degradation in aqueous solutions by ultrasound-assisted heterogeneous electro-Fenton process: Key operating parameters, mineralization and toxicity assessment. *Sep. Purif. Technol.* **2021**, *266*, 118533. [[CrossRef](#)]
15. Ziati, M.; Khemmari, F.; Aitbara, A.; Hazourli, S. Reduction of Turbidity and Chromium Content of Tannery Wastewater by Electrocoagulation Process: Ziati et al. *Water Environ. Res.* **2018**, *90*, 598–603. [[CrossRef](#)] [[PubMed](#)]
16. Mahmud, M.K.N.; Rozainy, M.M.R.; Abustan, I.; Baharun, N. Electrocoagulation process by using aluminium and stainless steel electrodes to treat total chromium, colour and turbidity. *Procedia Chem.* **2016**, *19*, 681–686. [[CrossRef](#)]
17. Loukanov, A.; El Allaoui, N.; Omor, A.; Elmadani, F.Z.; Bouayad, K.; Nakabayashi, S. Large-scale removal of colloidal contaminants from artisanal wastewater by bipolar electrocoagulation with aluminum sacrificial electrodes. *Results Chem.* **2020**, *2*, 100038. [[CrossRef](#)]
18. Marmanis, D.; Emmanouil, C.; Fantidis, J.; Thysiadou, A.; Marmani, K. Description of a Fe/Al Electrocoagulation Method Powered by a Photovoltaic System, for the (Pre-) Treatment of Municipal Wastewater of a Small Community in Northern Greece. *Sustainability* **2022**, *14*, 4323. [[CrossRef](#)]
19. Chen, G. Electrochemical technologies in wastewater treatment. *Sep. Purif. Technol.* **2004**, *38*, 11–41. [[CrossRef](#)]
20. Ikhlaiq, A.; Javed, F.; Akram, A.; Rehman, A.; Qi, F.; Javed, M.; Mehdi, M.J.; Waheed, F.; Naveed, S.; Aziz, H.A. Synergic catalytic ozonation and electroflocculation process for the treatment of veterinary pharmaceutical wastewater in a hybrid reactor. *J. Water Process. Eng.* **2020**, *38*, 101597. [[CrossRef](#)]
21. Asaithambi, P.; Aziz, A.R.A.; Daud, W.M.A.B.W. Integrated ozone—Electrocoagulation process for the removal of pollutant from industrial effluent: Optimization through response surface methodology. *Chem. Eng. Process. Process. Intensif.* **2016**, *105*, 92–102. [[CrossRef](#)]
22. Jin, X.; Xie, X.; Liu, Y.; Wang, Y.; Wang, R.; Jin, P.; Yang, C.; Shi, X.; Wang, X.C.; Xu, H. The role of synergistic effects between ozone and coagulants (SOC) in the electro-hybrid ozonation-coagulation process. *Water Res.* **2020**, *177*, 115800. [[CrossRef](#)] [[PubMed](#)]
23. Li, G.; Yang, C.; Yao, Y.; Zeng, M. Electrocoagulation of chromium in tannery wastewater by a composite anode modified with titanium: Parametric and kinetic study. *Desalin Water Treat* **2019**, *171*, 294–301. [[CrossRef](#)]
24. Elabbas, S.; Ouazzani, N.; Mandi, L.; Berrekhis, F.; Perdicakis, M.; Pontvianne, S.; Pons, M.N.; Lapique, F.; Leclerc, J.P. Treatment of highly concentrated tannery wastewater using electrocoagulation: Influence of the quality of aluminium used for the electrode. *J. Hazard. Mater.* **2016**, *319*, 69–77. [[CrossRef](#)]
25. Barrera-Díaz, C.; Bernal-Martínez, L.A.; Natividad, R.; Peralta-Hernández, J.M. Synergy of electrochemical/O<sub>3</sub> process with aluminum electrodes in industrial wastewater treatment. *Ind. Eng. Chem. Res.* **2012**, *51*, 9335–9342. [[CrossRef](#)]

26. Alam, R.; Sheob, M.; Saeed, B.; Khan, S.U.; Shirinkar, M.; Frontistis, Z.; Basheer, F.; Farooqi, I.H. Use of electrocoagulation for treatment of pharmaceutical compounds in water/wastewater: A review exploring opportunities and challenges. *Water* **2021**, *13*, 2105. [[CrossRef](#)]
27. Aber, S.; Amani-Ghadim, A.; Mirzajani, V. Removal of Cr (VI) from polluted solutions by electrocoagulation: Modeling of experimental results using artificial neural network. *J. Hazard. Mater.* **2009**, *171*, 484–490. [[CrossRef](#)]
28. Hakizimana, J.N.; Gourich, B.; Chafi, M.; Stiriba, Y.; Vial, C.; Drogui, P.; Naja, J. Electrocoagulation process in water treatment: A review of electrocoagulation modeling approaches. *Desalination* **2017**, *404*, 1–21. [[CrossRef](#)]
29. Gonzalez-Galvis, J.P.; Narbaitz, R.M. Large batch bench-scale dissolved air flotation system for simulating full-scale turbidity removal. *Environ. Technol.* **2020**, *43*, 1791–1804. [[CrossRef](#)]
30. Jin, X.; Zhang, L.; Liu, M.; Hu, S.; Yao, Z.; Liang, J.; Wang, R.; Xu, L.; Shi, X.; Bai, X.; et al. Characteristics of dissolved ozone flotation for the enhanced treatment of bio-treated drilling wastewater from a gas field. *Chemosphere* **2022**, *298*, 134290. [[CrossRef](#)]
31. Yao, Z.; Jin, X.; Liang, J.; Wang, R.; Jin, P.; Li, G.; Yao, L.; Wang, Z. Application of an integrated dissolved ozone flotation process in centralised fracturing wastewater treatment plant. *Water Reuse* **2021**, *11*, 236–247. [[CrossRef](#)]
32. Wang, J.; Wang, L.; Xu, S.; Ji, B.; Long, X. Experimental investigation on the cavitation performance in a venturi reactor with special emphasis on the choking flow. *Exp. Therm. Fluid Sci.* **2019**, *106*, 215–225. [[CrossRef](#)]
33. Fukui, Y.; Yuu, S. Removal of colloidal particles in electroflotation. *AIChE J.* **1985**, *31*, 201–208. [[CrossRef](#)]
34. Skoog, D.A.; West, D.M.; Holler, F.J.; Crouch, S.R. *Fundamentals of Analytical Chemistry*; Cengage Learning: Boston, MA, USA, 2013.
35. Sivagami, K.; Sakthivel, K.; Nambi, I.M. Advanced oxidation processes for the treatment of tannery wastewater. *J. Environ. Chem. Eng.* **2018**, *6*, 3656–3663. [[CrossRef](#)]
36. Umbarila-Ortega, M.F.; Prado-Rodríguez, J.S.; Agudelo-Valencia, R.N. Remoción de sulfuro empleando ozono como agente oxidante en aguas residuales de curtiembres. *Rev. Fac. de Ing.* **2019**, *28*, 25–38. [[CrossRef](#)]
37. Vakil, K.A.; Sharma, M.K.; Bhatia, A.; Kazmi, A.A.; Sarkar, S. Characterization of greywater in an Indian middle-class household and investigation of physicochemical treatment using electrocoagulation. *Sep. Purif. Technol.* **2014**, *130*, 160–166. [[CrossRef](#)]
38. Lin, C.J.; Lo, S.L.; Kuo, C.Y.; Wu, C.H. Pilot-scale electrocoagulation with bipolar aluminum electrodes for on-site domestic greywater reuse. *J. Environ. Eng.* **2005**, *131*, 491–495. [[CrossRef](#)]
39. El-Ashtoukhy, E.; Amin, N.; Fouad, Y. Treatment of real wastewater produced from Mobil car wash station using electrocoagulation technique. *Environ. Monit. Assess.* **2015**, *187*, 628. [[CrossRef](#)]
40. Emamjomeh, M.M.; Sivakumar, M. An empirical model for defluoridation by batch monopolar electrocoagulation/flotation (ECF) process. *J. Hazard. Mater.* **2006**, *131*, 118–125. [[CrossRef](#)]